Influence of nanographene platelets (NGP) incorporation on Fe_3O_4 nanoparticles as materials additives for enhancement thermal properties stearic acid

M. K. Nuryadin[1,2], R. Andiarto[1,2], A. Taufik[1,2], R. Saleh[1,2,*]

[1]Departemen Fisika, Fakultas MIPA-Universitas Indonesia, 16424 Depok, Indonesia

[2]Integrated Laboratory of Energy and Environment, Fakultas MIPA-Universitas Indonesia, 16424 Depok, Indonesia

[*]E-mail: rosari.saleh@ui.ac.id

Abstract. In this work, Fe_3O_4 nanoparticles, and Fe_3O_4/NGP composite were used as material additive for enhancement thermal properties of stearic acid (SA). The both material additive were synthesized using sol-gel method. Phase change material (PCM) composites SA-Fe_3O_4 and Sa-Fe_3O_4/NGP mixtures were made through the dispersion technique with three different weight % ratio of material additives into stearic acid: 1 wt.%, 3 wt.%, and 5 wt.%. X-Ray Diffractometer (XRD) and Fourier Transform Infrared (FTIR) spectroscopy were used to investigate the structural properties. Magnetic properties also measured by vibrating sample magnetometer (VSM) to see influence of NGP in PCM composites. Differential Scanning Calorimetry (DSC) and Thermogravimetric Analysis (TGA) were used in order to analyse the thermal properties of the samples. The results show an enhancement of the latent heat, thermal stability as well as specific heat by the presence of material additives in SA. Compare to SA-Fe_3O_4, SA-Fe3O4/NGP show better improvement in enhancement of thermal performance of SA. The improvement by about 41.2 % in specific heat and 21.2% in latent heat.

1. Introdcution

Thermal energy storage (TEM) has attracted more attention due to its heating and cooling application for waste heat recovery, solar thermal energy utilization and thermal management of electronics [1-3]. The variety of phase change material (PCM) especially the organic phase change material has been widely studied and has become the key technologies in the thermal energy storage application. Stearic acid which the common preferred organic phase change material is typically used due to their nontoxic, high energy storage density, thermal stability, and inconspicuous volume change [4-6]. Unfortunately, most of the organic phase change material including the stearic acid have a very low thermal conductivity which can limit their application. Therefore, some various methods are proposed in order to overcome this problem and one of the most promising method is by dispersing the nanoparticle into the PCM itself [7-9].

Adapting the idea of nanofluid, the nanomaterial utilization into the PCM is considered as a promising solution to enhance the thermal ability of the PCM in order to absorb and release heat [10]. A recent researchs show that the addition of the high thermal properties metal oxides such as Fe_3O_4, TiO_2 into the PCM has produced an enhancement in both latent heat and thermal conductivity [11-13]. Not only metal oxide, graphene with nano-sized material also shows a tremendous effect to the thermal

Content from this work may be used under the terms of the Creative Commons Attribution 3.0 licence. Any further distribution of this work must maintain attribution to the author(s) and the title of the work, journal citation and DOI.
Published under licence by IOP Publishing Ltd

properties of the PCM. For an example a research by Harish et.al [14] shows that the addition of the single-walled carbon nanohorn into the PCM has produced an increment into the thermal conductivity as well as its thermal latent heat. But unfortunately, there are only a few researches that investigate the addition of metal-oxide and graphene combination into the PCM. Therefore, in this research, Sa/Fe_3O_4 and Sa/Fe_3O_4/NGP are dispersed into the stearic acid and both of structural and thermal properties were observed.

2. Experimental

In this work, Iron (II) sulfate heptahydrate ($FeSO_4$. $7H_2O$, 99), sodium hydroxide (NaOH), nanoraphene platelets (NGP), and Stearic acid (Sa) as a phase change material are used without further purification. Fe_3O_4 nanoparticle prepared by using the same method as our previous study [15] while the Fe_3O_4/NGP with 10% NGP is prepared by sol-gel method. In brief, the NGP is dissolved in 80 ml of distilled water and 40 ml ethanol by using the ultrasonic treatment. The resulted 10% NGP solution is mixed into the 2 gram of Fe_3O_4 and are stirred for 2 h. The homogeneous suspension then is heated in the 120^{o}C for 3h or 3 h to affect the deposition on the graphene sheets. The resulting nanocomposite is isolated by centrifugation and dried in vacuum at 70 °C for 12 h. The PCM mixtures of Sa/Fe_3O_4 and Sa/ Fe_3O_4/NGP composites are prepared by dispersing the additives materials in the Sa with ultrasonic water bath for 2 hours. The ratio of Fe_3O_4 nanoparticle and Fe_3O_4/NGP nanocomposite were varied by 1, 3, and 5 wt% with the stearic acid.

The structural properties and chemical structures of all the samples are measured by the X-Ray Diffraction (XRD) and Fourier Transform Infrared (FTIR) respectively while the magnetic behaviors of the sample are measured by the vibrating sample magnetometer (VSM) measurement. For the thermal properties, Differential Scanning Calorimetry (DSC) is used in order to know the phase change behavior and specific heat capacity of the samples while the Thermo-gravimetric Analysis (TGA) is used to observe the degradation process of the samples.

3. Results and discussion

The XRD spectrum of Sa, Fe_3O_4 and NGP are plotted in Figure 1(a) along with the spectrum of Sa/Fe_3O_4 and Sa/Fe_3O_4/NGP with 5 wt% ratio as a representation of the Sa mixtures. The XRD pattern of the Sa shows the presence of two high peaks below the 2θ = 25°. These peaks are due to Sa crystallization peak. Another pattern from the XRD spectra of Fe_3O_4 confirms the inverse cubic spinel phase form at 2θ = 30.2°, 35.5°, 53.4°, and 57.0° which are attributed to the (220), (311), (511), and (440) crystalline planes. The strong diffraction pattern is also shown at 2θ = 26° for the (200) crystalline plane of NGP. The peaks of the Fe_3O_4 as well as the peaks of Sa can be obviously seen in the XRD spectra of Sa/Fe_3O_4 and Sa/Fe_3O_4/NGP with the additional NGP peak in the spectra. The XRD results indicate that all of the samples are consisted of the desired materials.

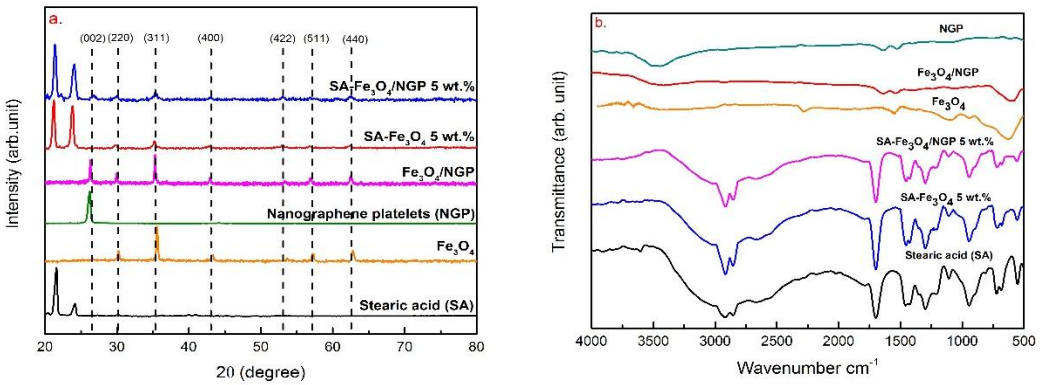

Figure 1. (a) XRD patterns and (b) FTIR spectrum of SA, Fe3O4, NGP, Fe3O4/NGP SA-Fe3O4 wt. % and SA-Fe3O4/NGP 5 wt.%.

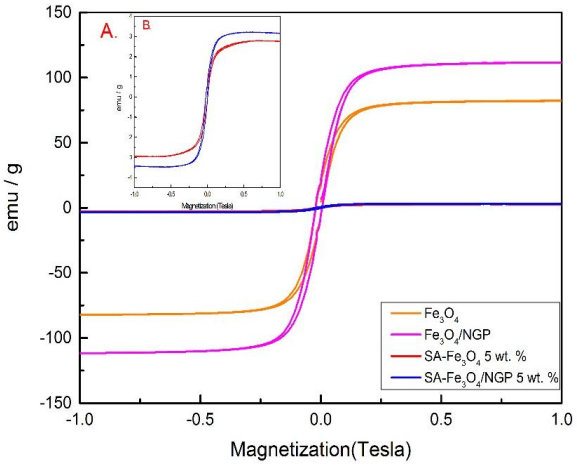

Figure 2. VSM Spectra of (a) Fe_3O_4, Fe_3O_4/NGP, SA-Fe_3O_4 and SA-$Fe_3O_4$4/NGP and (b) SA-Fe_3O_4 and SA-Fe_3O_4/NGP

Table.1 Magnetic Saturation of Fe_3O_4, Fe_3O_4/NGP, SA-Fe_3O_4 and Fe_3O_4/NGP

Sample	M-S (emu/g)
Fe_3O_4	82
Fe_3O_4/NGP	112
SA-Fe_3O_4 5 wt.%	2.76
SA-Fe_3O_4/NGP 5 wt. %	3.16

Figure 1(b) shows the FTIR transmittance pattern of Sa, Sa-Fe_3O_4, and Sa-Fe_3O_4/NGP. The transmittance pattern of Sa shows the strong absorption bands at 2917 cm^{-1}, 2849 cm^{-1} and 1703 cm^{-1} which are attributed to the stretching vibration of $–CH_3$, $–CH_2$ and C=O molecules respectively while another absorption bands at 1464 cm^{-1}, 1296 cm^{-1}, 934 cm^{-1} and 720 cm^{-1} correspond to in plane, out of plane and in plane swinging of OH molecules [16]. There are no transmittance pattern of the Fe_3O_4 and NGP that can be seen in the Sa-Fe_3O_4, and Sa-Fe_3O_4/NGP due to the small amount of the additives materials. However, the similar transmittance pattern of the Sa in Sa/Fe_3O_4 and Sa/Fe_3O_4/NGP spectra indicate that there are no chemical pattern takes place between the PCM and the additives.

The magnetic hysteresis curve of Sa/Fe_3O_4 and Sa/Fe_3O_4/NGP alongside with Fe_3O_4 and Fe_3O_4/NGP as the additive materials are plotted in Figure 2. The magnetic saturation values are also listed in the Table 1. The magnetic behaviour of Fe_3O_4 is increased with the presence of the NGP particles. The same tendency is also observed for Sa/Fe_3O_4 and Sa/Fe_3O_4/NGP with the smaller magnetic saturation due to the small amount of the Fe_3O_4 nanoparticle and Fe_3O_4/NGP nanocomposite in the Sa.

For the thermal degradation process, the TGA measurements results of the Sa/Fe_3O_4 (Figure 3(a)) and Sa/Fe_3O_4/NGP (Figure 3(b)) show that the Sa begins to decompose at about 200^oC. However, the slightly change in temperature decomposition are found in the Sa/Fe_3O_4 samples and are more distinguishable in the Sa/Fe_3O_4/NGP samples. Higher temperature decomposition process can provides the higher thermal stability on the PCM which is very important to the thermal energy storage. The TGA measurement also shows the information about the residual weight composition of the sample after the decomposition process. The percentage loss of Sa in Table 2 corresponds to the composition of the samples Sa/Fe_3O_4 and Sa/Fe_3O_4/NGP. DSC curve of the Sa/Fe_3O_4 and Sa/Fe_3O_4/NGP with 1, 3, and 5wt% ratios are shown in Fig. 4a and Fig. 4b respectively in order to know the melting and solidifying process of the Sa composites as the PCM. The melting and solidifying points of the samples from the DSC curves are tabulated in Table 3 along with the latent heat values. The presence of the Fe_3O_4 and Fe_3O_4/NGP do not cause any favourable effect on the melting and solidification

point. The Sa completely melt at temperature 70.5 ^{o}C while its solidifying temperature is 66 ^{o}C. The slightly change occurs in the melting and solidifying temperature for the Sa/Fe_3O_4 and Sa/Fe_3O_4/NGP. Both latent heat of melting and solidifying are higher for Sa/Fe_3O_4 and Sa/Fe_3O_4/NGP than that of Sa. The enhancement of the latent heat can be explained with molecular attraction between Sa and the nanocomposite [17-18]. The influence of the addition of Fe_3O_4 and Fe_3O_4/NGP on enhancing the value of latent heat showed the enhancement ability of the Sa composites to absorb and release heat with greater energy capacity.

The specific heat values of the samples are also calculated from the DSC results and are plotted in

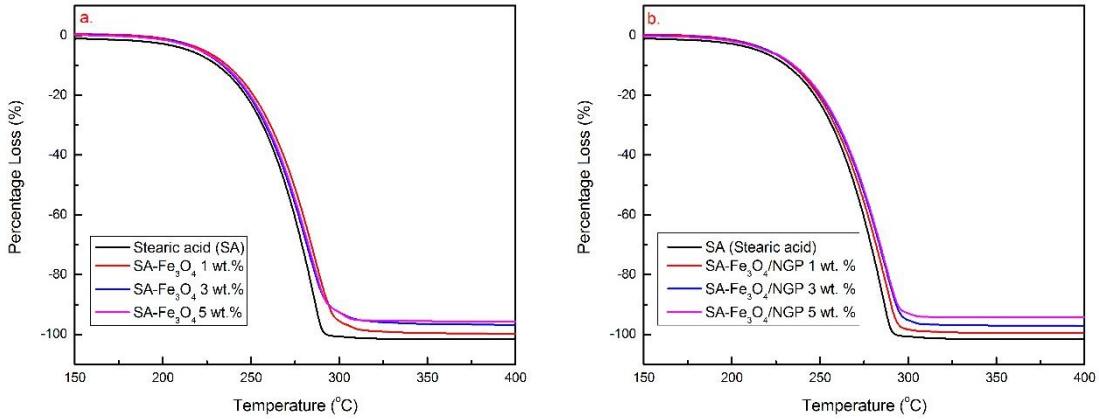

Figure 3. TGA (a) SA-Fe3O4 5 wt. % various wt. % and (b) SA-Fe_3O_4/NGP various wt. %

Table 2. TGA result of SA- Fe_3O_4 5 wt. % various wt. % and SA- Fe_3O_4/NGP various wt. %

Sample	Onset Temp	Percentage Loss
Stearic acid (SA)	251.6°C	100%
SA-Fe_3O_4 1 wt.%	251.4°C	99.89%
SA-Fe_3O_4 3 wt.%	250.2°C	96.41%
SA-Fe_3O_4 5 wt.%	251.6°C	94.49%
SA-Fe_3O_4/NGP 1 wt. %	253.5°C	99.19
SA-Fe_3O_4/NGP 3 wt. %	253.6°C	96.99
SA-Fe_3O_4/NGP 5 wt. %	254.2°C	94.17

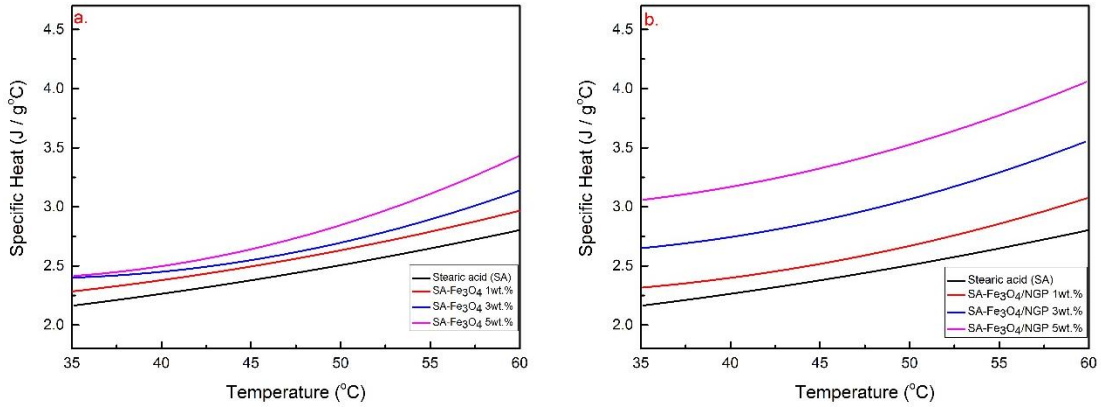

Figure 4. Specific heat of solid polynomial fitting curve (a) SA-Fe3O4 various wt. % and (b) SA-Fe3O4/10% NGP various wt. %

Table 3. DSC result of SA-Fe_3O_4 5 wt. % various wt. % and SA-Fe_3O_4/10% NGP various wt. %

Sample	Solid-liquid			Liquid-solid		
	T_{onset}	T_{peak}	T_{endset}	T_{onset}	T_{peak}	T_{endset}
Stearic acid (SA)	67.5	70.5	76	67.2	66.6	63.1
SA-Fe_3O_4 1 wt.%	67.53	70.48	76.1	66.26	66.72	62.81
SA-Fe_3O_4 3 wt.%	67.52	70.16	75.8	65.88	66.83	62.74
SA-Fe_3O_4 5 wt.%	67.4	70.4	76.1	64.6	66.6	62.2
SA-Fe_3O_4/10% NGP 1 wt. %	67.78	70.57	76.2	67.84	66.73	63.16
SA-Fe_3O_4/10% NGP 3 wt. %	67.61	70.43	76.1	67.89	66.7	63.24
SA-Fe_3O_4/10% NGP 5 wt. %	67.63	70.42	75.9	67.89	66.8	63.45

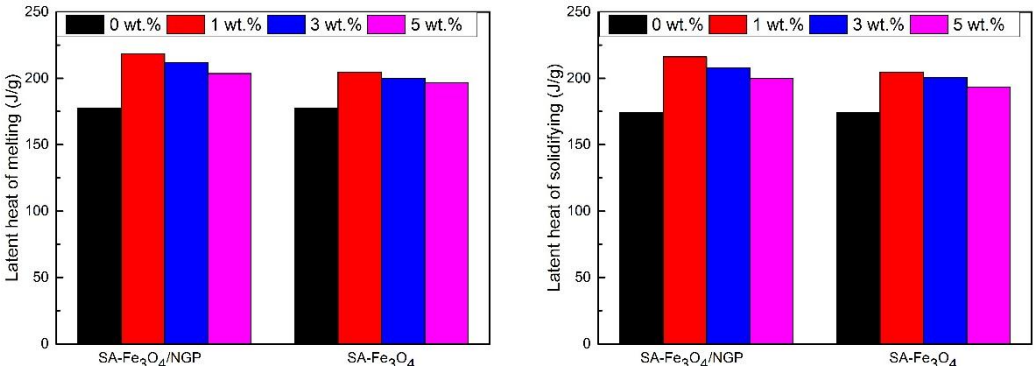

Figure 5. Latent heat melting proses and solidifying proses.

the Figure 4(a) and Figure 4(b) for the Sa/Fe_3O_4 and Sa/Fe_3O_4/NGP respectively. The result showed that Fe_3O_4 nanoparticles increase the specific heat value of Sa and further increase for Fe_3O_4/NGP. The value of specific heat also increase as with the addition of weight percent of the Fe_3O_4 added to either with or without NGP. The enhancement of specific heat indicates that the addition of the Fe_3O_4 and Fe_3O_4/NGP in the Sa also enhance the ability of the Sa in the sensible heat condition.

The comparison of latent heat storage between pure SA and PCM composites and also data of characterization are tabulated in Table 3. In charging process both PCM composites in onset, peak, and endset temperature do not significantly change from pure SA. On the other hand in discharging process, PCM composites shows difference behaviour in onset temperature from pure SA. In SA-Fe_3O_4 discharging curve shows that onset temperature become more smaller with increasing Fe_3O_4 wt.%. While in SA-Fe_3O_4/NGP discharging process curve shows a small increases in onset temperature. It is shows that small amount of NGP in Fe_3O_4/NGP can maintain the onset temperature of pure stearic acid. In Figure 5 plotted latent heat storage charging and discharging process of PCM composites. From Figure 6 shows that latent heat storage of samples increases with content of material additives various wt. %. Maximum enhancement of latent heat PCM composites occurs in content material additives at 1 wt.%. The enhancement of latent heat of SA-Fe_3O_4/NGP shows higher improvement than SA-Fe_3O_4. Latent heat of SA-Fe_3O_4/NGP improved by about 23% while SA-Fe_3O_4 improved by 15%. The enhancement of latent heat storage PCM composite is due to molecular interaction between molecules SA and material additives. Molecular interactions between molecules and material additives is physical interactions that are affected by the large surface area of material additives. The larger surface area of material additives produces greater interaction molecular with molecules SA [18-20]. From the result of XRD spectra Fe_3O_4/NGP have smaller crystallite size than Fe_3O_4 that can be lead to increased surface area. Therefore the enhancement of latent heat SA with addition Fe_3O_4/NGP have better improvement than Fe_3O_4.

4. Conclusion

Fe_3O_4 nanoparticles and Fe_3O_4/NGP nanocomposites were synthesized using sol gel method and used as material additives into PCM composites various wt. % prepared by dispersion using sonication method. Material additives used as enhancement latent heat storage of stearic acid. Based on XRD synthesized PCM composite shows that crystal structure SA and material additives remain unchanged. Thermal stability of SA-Fe_3O_4/NGP slightly increase than SA because the incorporation of NGP in nanocomposites. Enhancement of specific heat and latent heat storage were confirmed via DSC curve show that both of Fe_3O_4 and Fe_3O_4/NGP increased thermal performance of SA. In comparison material additives for percentage of enhancement specific heat and latent heat storage of SA, Fe_3O_4/NGP have higher improvement than Fe_3O_4 because of small content NGP in nanocomposites.

5. References

[1] Sharma A, Tyagi VV, Chen CR, et al. 2009 *Renewable and Sustainable Energy Reviews* **13** 318-345
[2] Farid MM, Khudhair AM, Razack SAK, et.al. **2004** *Energy Conservation and management* **45** 1597-1615
[3] Zalba B, Marin JM, Cabeza LF, et al. 2003 *Applied Thermal Engineering* **23** 251-283
[4] Li B, Liu T, Hu L, Wang Y, and Nie S 2013 *Chemical Engineering* **215** 819-826
[5] Cao L, Tang Y and Fang G 2014 *Energy* **80** 98-103
[6] Chen Z, Cao L, Fang G 2013 *Energy and Buildings* **62** 469-474
[7] Agyenim F, Hewitt N, Eames P, Smyth M. 2010 *Renewable & Sustainable Energy Reviews* **14** 615–628
[8] Sahan N and Paskoy HO 2014 *Solar Energy Materials & Solar Cells* **126** 56-61
[9] Teng TP and Cheng CM 2013 *Applied Thermal Engineering* **50** 637-644
[10] Kim S and Drzal LT 2009 *Solar Energy Materials and Solar Cells* **93** 136–142
[11] Elgafy A and Lafdi K 2005 *Carbon* **43** 3067-3074.
[12] Li Y, Zhu J, Wei S, Ryu J, Sun L, and Macromol ZG 2011 *Chemicals Physics* **212** 1951-1959.
[13] Arifin SA, Jalaludin S, and Saleh R 2015 *Advanced Materials research* **1123** 264-269
[14] Taufik A and Saleh R 2016 *Materials Science Forum* **1725** 020089
[15] Andiarto R, Nuryadin MK,and Saleh R 2016 *Journal of Physics: Conference Series* **710** 012020
[16] Harikrishnan S, Magesh S and Kalaiselvam S 2013 *Thermochimica Acta* **565** 137-145
[17] Cao Y, Feng J and Wu P 2010 *Carbon* **48** 3834–3839
[18] Shaikh S, Lafdi K and Hallinan K 2008 *Journal of Applied Physics* **103** 094302
[19] Şahan, Fois M and Paksoy H 2015 *Solar Energy Materials and Solar Cells* **137** 61–67
[20] Warzoha RJ and Fleischer AS2014 *International Journal of Heat and Mass Transfer* **79** 314-323